An Epiallele at *cly1* Affects the Expression of Floret Closing (Cleistogamy) in Barley

Ning Wang,[1] Shunzong Ning, Jianzhong Wu, Akemi Tagiri, and Takao Komatsuda[2]
National Institute of Agrobiological Sciences (NIAS), Plant Genome Research Unit, 2-1-2 Kannondai, Tsukuba, Ibaraki 305-8602, Japan

ABSTRACT The swelling of the lodicule is responsible for floret opening in many grass species, allowing for pollen dispersal and cross-pollination. In barley, the closed floret habit (cleistogamy) is under the control of *cly1*, a gene that operates by inhibiting the development of the lodicule. In non-cleistogamous cultivars, *cly1* mRNA is degraded by miR172-directed cleavage, allowing the lodicules to swell; however, in cultivars carrying the recessive allele *cly1.b*, a single-nucleotide substitution destroys the miR172 target site preventing mRNA cleavage. Barley cv. SV235 is cleistogamous; its *cly1* coding sequence is identical to that of *cly1.b*, but its lodicules do develop, although insufficiently to produce a non-cleistogamous flower. In this cultivar, the downregulation of *cly1* is unrelated to miR172-directed mRNA degradation, but rather is caused by an epiallele that represses transcription. Allelic relationships between known *cly1* alleles were explored by the quantification of lodicule vascularization and an assessment of the response of the spike to the supply of exogenous auxin. The SV235 phenotype can be manipulated by a pre-anthesis application of 2,4-D, a feature that could be of interest in the context of hybrid barley grain production based on cleistogamy.

THE swelling of the lodicule, a structure found in the floret of many grass species and functionally related to the petal in the hermaphroditic angiosperm flower, drives apart the palea and lemma, thereby opening the floret so that it can release its pollen and be readily cross-pollinated (Briggs 1978). In barley, closed flowering (cleistogamous) variants are known. In some of these, the lodicule fails to swell (Kurauchi *et al.* 1994; Turuspekov *et al.* 2004; Honda *et al.* 2005; Wang *et al.* 2013). The *cleistogamy 1* gene (*cly1*) has been shown to encode an AP2-protein and is a paralog of *HvAP2-like* in barley and *Q* in bread wheat (Simons *et al.* 2006; Nair *et al.* 2010; Simonov and Pshenichnikova 2012; Ning *et al.* 2013). In non-cleistogamous barleys, *cly1* mRNA is cleaved by an miRNA, with the result that the abundance of full-length gene product remains at a low level. Two cleistogamy alleles are known, *cly1.b* and *cly1.c*; in both cases, *cly1* mRNA is not cleaved by miR172, resulting in the failure of the lodicule to swell. Exceptionally, in cv. SV235, although its *cly1* coding sequence is identical to that of *cly1.b*, its lodicules do swell at anthesis, although insufficiently to force open the floret. Here, we show the genetic and epigenetic basis of the unusual lodicule development seen in cv. SV235.

doi: 10.1534/genetics.114.171652
Manuscript received June 14, 2014; accepted for publication October 20, 2014; published Early Online November 13, 2014.
Supporting information is available online at http://www.genetics.org/lookup/suppl/doi:10.1534/genetics.114.171652/-/DC1.
[1]Present address: Faculty of Life and Environmental Sciences, University of Tsukuba, 1-1-1 Tennoudai, Tsukuba, Ibaraki, 305-8577, Japan.
[2]Corresponding author: National Institute of Agrobiological Sciences (NIAS), Plant Genome Research Unit, 2-1-2 Kannondai, Tsukuba, Ibaraki 305-8602, Japan. E-mail: takao@affrc.go.jp

Materials and Methods

Plant materials

Grain of the barley cultivars SV002 (OUA008, "Sanalta"), SV223 (OUU059, "Tammi"), SV230 (OUU305, "Badajoy"), SV235 (OUU326, "France 1"), SV237 (OUU329, "Cygne"), SV241 (OUU351, "Plumage"), SV242 (OUU352, "Imperial"), and SV255 (OUU613, "Otello"), along with the *Hordeum vulgare* subsp. *spontaneum* accession OUH602 (the OU numbers relate to the Barley and Wild Plant Resource Center collection, http://www.rib.okayama-u.ac.jp/barley/index.html), was obtained from the Institute of Plant Science and Resources, Okayama University, Kurashiki, Japan. The SV numbers represent designators within a core collection designed to capture the global diversity of barley (Saisho *et al.* 2009; Nair *et al.* 2010). Grain of the cultivars "Azumamugi" (AZ), "Kanto Nakate Gold" (KNG), and "Golden Promise" (GP) were supplied by the NIAS Gene Bank, Tsukuba, Japan, that of

"Satsuki Nijo" (SN) by K. Matsui (National Institute of Crop Science, Tsukuba, Japan), that of "Barke" (BAR) by N. Stein (Leibniz Institute of Plant Genetics and Crop Plant Research, Gatersleben, Germany), and that of "Morex" (MOR) by A. Kleinhofs (Department of Crop and Soil Sciences and School of Molecular Biosciences, Washington State University, Pullman, WA). Plants were sown during the fall in the field at Tsukuba, spaced 20 cm apart in rows separated from one another by 80 cm.

Histological analysis

Cross sections were made from immature spikes at the green anther stage (Kirby and Appleyard 1981) by fixing overnight at 4° in 4% w/v paraformaldehyde/0.25% w/v glutaraldehyde in 50 mM sodium phosphate buffer (pH 7.2), followed by dehydration through first a graded ethanol series and then a *t*-butanol series, and finally embedded in Paraplast Plus (Kendall, Mansfield, MA). Microtome sections (8–10 μm thick) were mounted on amino silane coated glass slides (Matsunami Glass, Osaka, Japan). The sections were deparaffinized in xylene, hydrated through a graded ethanol series to distilled water, and stained in toluidine blue O.

Measurement of lodicule size

At least three spikes per accession were sampled at the yellow anther stage (Kirby and Appleyard 1981). Lodicules in florets sampled from the central portion of the spike were photographed after the removal of the lemma, and the resulting images were used to measure lodicule width and depth as surrogates of lodicule volume, following Nair *et al.* (2010). In addition, the width and depth of the transparent portion (Supporting Information, Figure S1) were used as a metric of lodicule vascularization. Culm was cut under the flag leaf node and the response of the lodicule to 2,4-D treatment (100 mg/liter) at room temperature was assessed after 3 days, following Honda *et al.* (2005).

Linkage analysis

Sets of 96 F_2 progeny were generated from each of the crosses SV235 × KNG, × SV223, and × SV230. A localized genetic map was constructed based on STS assays derived from the RFLP loci *ABC165* and *ABC153*, following Turuspekov *et al.* (2004) and used for QTL detection via Windows QTL Cartographer v. 2.5 software (Wang *et al.* 2012), applying a LOD threshold of 3.0. The CAPS marker AP2CAPS2743SacI was developed to distinguish a sequence variant in the ninth intron of *cly1* (Table S3). The primer pair BF623536U236M060H23U613/BF623536U514M060H23L794 (Nair *et al.* 2010) was used to amplify a segment on the 3′ side of *cly1*. Each 10 μl PCR, containing 40 ng template, 0.5 U ExTaq DNA polymerase (Takara Bio Inc., Ōtsu, Japan), 1× PCR buffer, 2.0 mM $MgCl_2$, 200 μM dNTP, 10% DMSO, and 300 nM of each primer, was exposed to a 94°/5 min denaturation, followed by 35 cycles of 94°/30 sec, 60°/30 sec, and 72°/60 sec, with a final 72°/10 min extension. The CAPS reaction involved the addition of 2.5- to 5-unit *Sac*I (Nippon Gene, Tokyo, Japan) and 1× buffer. After holding for 6 hr at 37°, the reaction products were electrophoresed through 2% agarose gels and visualized by EtBr staining.

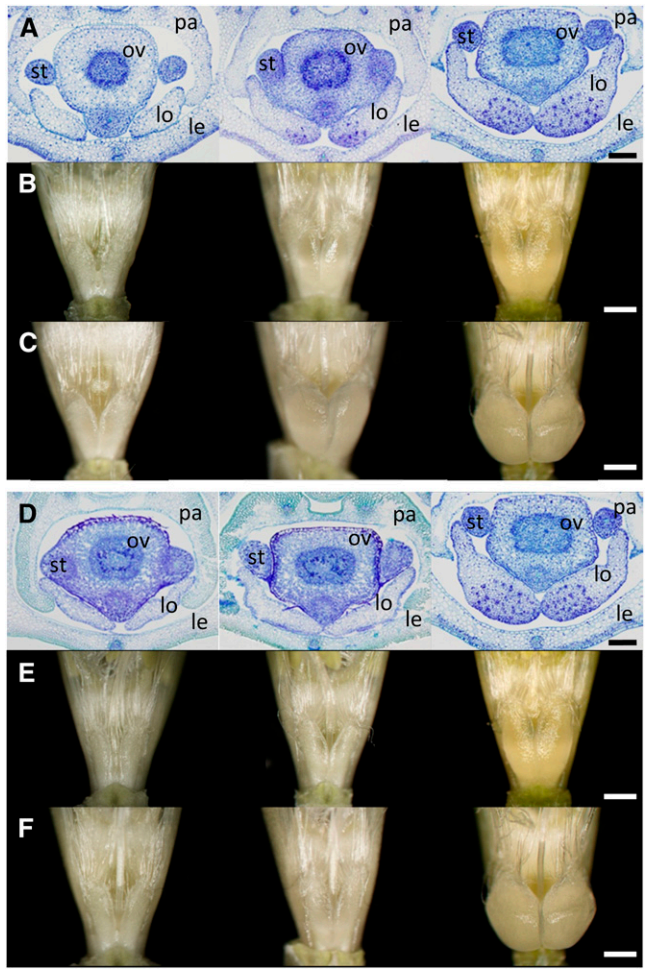

Figure 1 Lodicules of the cleistogamous barley cultivar SV235 (*cly1*.b2) and in its F_1 hybrids with cvs. KNG (*cly1*.b) and SV230 (*cly1*.c). (A–C) Left, KNG; middle, SV235 × KNG F_1 hybrid; right, SV235. (D–F) Left, SV230; middle, SV235 × SV230 F_1; right, SV235. (A and D) Transverse sections at the green anther stage. (B, C, E, and F) Stereomicroscope images. (B and E) Yellow anther stage, (C and F) Anthesis stage (spikes exposed to 100 ppm 2,4-D for 3 days). Scale bars: (A and D) 200 μm; (B, C, E, and F) 600 μm. Lodicule (lo), stamen (st), ovary (ov), lemma (le), and palea (pa).

Transcription analysis

Total RNA was extracted from a 30- to 100-mg sample taken from a bulk of 3–10 immature spikes (three biological replicates) using an RNAqueous kit (Ambion, Life Technologies, Tokyo, Japan). The resulting RNA was treated with RNase-free DNase I (Takara Bio Inc.) before being used as a template for the synthesis of single-strand cDNA using SuperScript III (Invitrogen, Life Technologies Japan, Tokyo) primed with either oligo(dT) or random primers. Primer pairs (900 nM of each forward and reverse primer) and the corresponding TaqMan probes (250 nM) specific to either *cly1* or *actin* (Wang *et al.* 2013) were used for quantitative real time PCR (qPCR) analyses, carried out on a StepOne Real-Time

Table 1 Lodicule size and anther extrusion (AE) measured in selected cultivars and intercultivar hybrids

Crosses	Width (mm)		Depth (mm)		AE in field	Response to 2,4-D	AE by 2,4-D
	Overall	Transparent	Overall	Transparent			
			Parents				
SV235 (*cly1.b2*)	0.55 ± 0.11	0.55 ± 0.11	0.43 ± 0.05	0.43 ± 0.05	–	+	+
AZ (*Cly1.a*)	0.72 ± 0.04	0.72 ± 0.04	0.56 ± 0.05	0.56 ± 0.05	+	+	+
SN (*Cly1.a*)	0.66 ± 0.05	0.66 ± 0.05	0.53 ± 0.03	0.53 ± 0.03	+	+	+
Morex (*Cly1.a*)	0.73 ± 0.01	0.73 ± 0.01	0.55 ± 0.01	0.55 ± 0.01	+	+	+
Barke (*Cly1.a*)	0.85 ± 0.05	0.83 ± 0.05	0.61 ± 0.03	0.60 ± 0.02	+	+	+
OUH602 (*Cly1.a*)	0.59 ± 0.02	0.59 ± 0.01	0.44 ± 0.04	0.44 ± 0.04	+	+	+
KNG (*cly1.b*)	0.47 ± 0.03	0.07 ± 0.01	0.29 ± 0.02	0.03 ± 0.01	–	–	–
GP (*cly1.b*)	0.48 ± 0.05	0.10 ± 0.03	0.31 ± 0.02	0.04 ± 0.01	–	–	–
SV002 (*cly1.b*)	0.50 ± 0.01	0.04 ± 0.04	0.25 ± 0.07	0.02 ± 0.02	–	–	–
SV242 (*cly1.b*)	0.45 ± 0.02	0.06 ± 0.02	0.24 ± 0.02	0.03 ± 0.01	–	–	–
SV223 (*cly1.c*)	0.42 ± 0.00	0.05 ± 0.01	0.21 ± 0.00	0.03 ± 0.00	–	–	–
SV230 (*cly1.c*)	0.35 ± 0.05	0.05 ± 0.01	0.14 ± 0.00	0.03 ± 0.00	–	–	–
			cly1.b2 × *Cly1.a*				
SV235 × AZ	0.72 ± 0.03	0.72 ± 0.03	0.50 ± 0.06	0.50 ± 0.06	+	+	+
SV235 × SN	0.69 ± 0.01	0.69 ± 0.01	0.50 ± 0.08	0.50 ± 0.08	+	+	+
SV235 × Morex	0.75 ± 0.07	0.75 ± 0.07	0.62 ± 0.11	0.62 ± 0.11	+	+	+
			cly1.b2 × *cly1.b*				
SV235 × KNG	0.54 ± 0.02	0.33 ± 0.05	0.44 ± 0.03	0.22 ± 0.02	–	+	–
SV235 × GP	0.59 ± 0.06	0.46 ± 0.00	0.43 ± 0.04	0.35 ± 0.03	–	+	–
SV235 × SV002	0.60 ± 0.02	0.34 ± 0.03	0.42 ± 0.06	0.21 ± 0.01	–	+	–
SV235 × SV242	0.55 ± 0.05	0.36 ± 0.04	0.44 ± 0.07	0.20 ± 0.04	–	+	–
			cly1.b2 × *cly1.c*				
SV235 × SV223	0.44 ± 0.05	0.07 ± 0.01	0.28 ± 0.03	0.07 ± 0.01	–	–	–
SV235 × SV230	0.44 ± 0.04	0.09 ± 0.01	0.23 ± 0.01	0.05 ± 0.02	–	–	–
			Cly1.a × *cly1.b*				
AZ× KNG	0.62 ± 0.04	0.61 ± 0.04	0.42 ± 0.06	0.42 ± 0.06	+	+	+
SN × KNG	0.59 ± 0.04	0.59 ± 0.03	0.41 ± 0.04	0.40 ± 0.04	+	+	+
SN× GP	0.61 ± 0.03	0.61 ± 0.03	0.43 ± 0.04	0.42 ± 0.04	+	+	+
Barke × KNG	0.72 ± 0.05	0.72 ± 0.04	0.51 ± 0.06	0.50 ± 0.06	+	+	+
			Cly1.a × *cly1.c*				
SV230 × SN	0.53 ± 0.05	0.52 ± 0.05	0.37 ± 0.08	0.35 ± 0.07	–	+	+
SV230 × Morex	0.51 ± 0.02	0.50 ± 0.01	0.38 ± 0.05	0.36 ± 0.05	–	+	+
Barke × SV230	0.55 ± 0.05	0.54 ± 0.05	0.36 ± 0.03	0.36 ± 0.03	–	+	+
SV230 × OUH602	0.54 ± 0.05	0.53 ± 0.03	0.35 ± 0.06	0.34 ± 0.06	–	+	+
			Cly1.c × *cly1.b*				
SV230 × KNG	0.43 ± 0.01	0.01 ± 0.01	0.25 ± 0.01	0.01 ± 0.01	–	–	–

Lodicule width: "overall" indicates entire size of width and depth at a visible lodicule and "transparent" indicates the width and depth of vascular tissue at a lodicule. AE, anther extrusion.

PCR System device (Applied Biosystems, Life Technologies, Tokyo, Japan), were based on TaqMan Gene Expression Master Mix (Applied Biosystems). The cycling regime consisted of a 60°/30-sec incubation, followed by a 95°/10 min denaturation, 40 cycles of 92°/30 sec, 60°/60 sec, and a final 60°/10-min extension. Transcript quantification was based on the $^{\Delta\Delta}C_T$ method (Livak and Schmittgen 2001). Transcript abundances have been presented as fold differences following normalization against the geometric mean of *actin* transcript levels relative to a calibrator sample (KNG at the lemma primordium stage).

The primer combination SV235-244RT_600U/SV235-244RT_712L (Table S1), designed to target a putative long noncoding RNA sequence (lncRNA) surrounding the −245/−244-nt CpG site in the *cly1* sequence, was used for a semi-quantitative RT–PCR assay. Each 10-μl PCR containing 2-μl cDNA template, 0.5 units ExTaq DNA polymerase (Takara Bio, Inc., Ōtsu, Japan), 1× PCR buffer, 2.0 mM $MgCl_2$, 200 μM dNTP, and 300 nM of each primer. The cycling consisted of a 95°/5-min denaturation, 40 cycles of 94°/30 sec, 55°/30 sec, 72°/30 sec and a final 72°/5-min extension.

Modified 5′-RACE

RNA ligase-mediated 5′-RACE was performed using a GeneRacer kit (Invitrogen). Total RNA was isolated from immature spikes at the awn primordium stage. The dephosphorylation and decapping steps were omitted to ensure that

only the 5′ ends of the truncated transcripts remained ligatable to the GeneRacer RNA oligomer. A nested PCR employed a primer targeting the GeneRacer RNA oligomer, initially in combination with the reverse gene specific primer, as described by Nair *et al.* (2010). Each PCR contained 30 ng template, 0.5 units ExTaq DNA polymerase (Takara Bio, Inc.), 1× buffer, 2.5 mM $MgCl_2$, 200 μM dNTP, and 300 nM of each primer. The initial PCR comprised a 94°/5-min denaturation, followed by five cycles of 94°/30 sec, 72°/2 min, five cycles of 94°/30 sec, 70°/2 min and 25 cycles of 94°/30 sec, 64°/30 sec, 72°/60 sec, with a final 72°/10-min extension. The second PCR comprised a 94°/5-min denaturation, followed by 25 cycles of 94°/30 sec, 65°/30 sec, 68°/60 sec, with a final 68°/10-min extension. Control reactions featured the cleavable allele *Cly1.a* from AZ. The amplicons were separated by agarose gel electrophoresis and cloned into the TA vector (Invitrogen). Randomly selected clones without size selection were taken forward for DNA sequencing.

Resequencing of cly1 alleles

DNA was extracted from each plant following Komatsuda *et al.* (1998). The primer pairs used to amplify an 11.2-kb region (which harbored 3.8 kb of 5′ sequence, 3.6 kb of the coding region, and 3.8 kb of 3′ sequence) have been described by Wang *et al.* (2013). For the purpose of sequencing, each 10 μl PCR was made up with 40 ng template, 0.5 units ExTaq DNA polymerase (Takara Bio, Inc.), 1× buffer, 2.5 mM $MgCl_2$, 200 μM dNTP, and 300 nM of each primer, and the cycling regime comprised a 94°/5-min denaturation step, followed by 35 cycles of 94°/30 sec, 55°/30 sec, 72°/60 sec, with a final 72°/10-min extension. The reaction products, purified using a QIAquick PCR Purification kit (Qiagen, Tokyo, Japan), provided the template for subsequent sequencing.

Bisulfite sequencing

Genomic DNA, isolated from immature spikes at the stamen primordium stage, the green anther stage, and from young leaves by means of a DNeasy Plant Mini kit (Qiagen), was bisulfite-treated (Kenan-Eichler *et al.* 2011) with the help of an EpiTect Bisulfite kit (Qiagen), following the manufacturer's protocol. DNA fragments were amplified using bisulfite primers (sequences listed in Table S1) and cloned into the pCR 2.1-TOPO vector (Invitrogen). The sequence of at least 16 clones per amplicon was acquired.

Deep sequencing of small RNAs

Small RNA-seq reads (Illumina, Tokyo, Japan) were obtained from the immature spikes of MOR at the lemma primordium, stamen primordium, and awn primordium stages. Total RNA was extracted using a mirVana miRNA Isolation kit (Life Technologies), following the manufacturer's instructions, and an Illumina mRNA-seq Sample Preparation kit was used to process ~5 μg of total RNA, following the manufacturer's protocol (part 1004898 Rev. D). The size range of RNAs captured to target 20- to 24-nt siRNA was 80–125 nt, since these RNAs have ligated with adaptor. Sequencing was performed

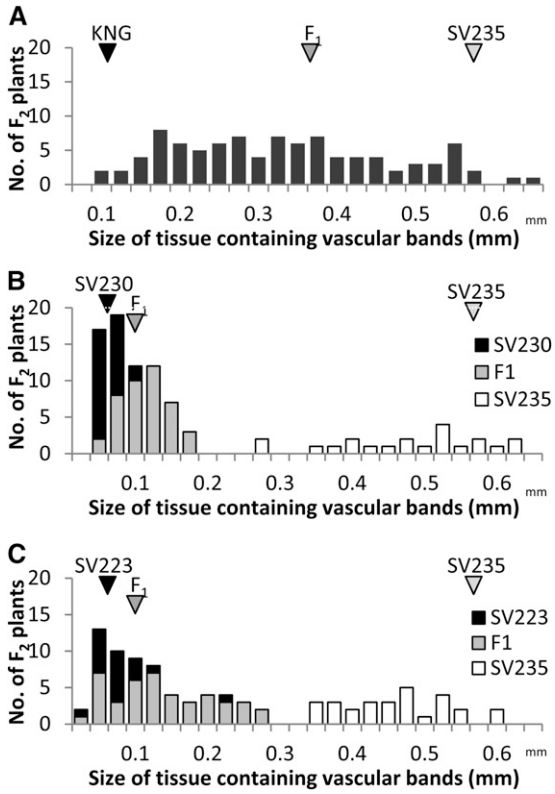

Figure 2 Distribution in the width of vascularized lodicule tissue. Bar colors represent genotype for the CAPS marker within *cly1*. (A) SV235 × KNG F_2 population (n = 94), (B) SV235 × SV230 F_2 population (n = 94), (C) SV235 × SV223 F_2 population (n = 92).

using an Illumina Genome Analyzer IIx, which generated 36-nt paired-end reads. An in-house program was used to trim low-quality bases (<Q15) from both the 5′ and 3′ ends of reads until a stretch of at least 3 nt of high-quality (≥Q15) bases was obtained. Illumina adapter sequences (5′ P-ATCTCGTATGCCGTCTTCTGCTTG) were removed by applying the "cutadapt" v. 1.0 routine (http://code.google.com/p/cutadapt/). Barley genome DNA sequence was obtained from ftp://ftpmips.helmholtz-muenchen.de/plants/barley/public_data/ and RNA-seq data from http://www.ebi.ac.uk/ena/data/view/ERR159679) (Mayer *et al.* 2012). siRNA reads were mapped against both the MOR whole genome sequence assembly (Mayer *et al.* 2012) and the sequence of the MOR BAC clone GQ40305, which harbors a 4-kb fragment of the *cly1* 5′ region and 3.5 kb of its coding region (Nair *et al.* 2010), using Bowtie 1 v. 0.12.8 (Langmead *et al.* 2009). mRNA reads of the RNA-seqdata were mapped using TopHat v. 2.0.4 (Trapnell *et al.* 2009).

Results

Natural variation for the development of the lodicule vascular bundles and for anther extrusion

As early as the green anther stage, SV235 lodicules were already significantly larger than those produced by either KNG (*cly1.b*) (Figure 1A) or SV230 (*cly1.c*) (Figure 1D). The

Table 2 Patterns of segregation in the F2 generation bred from intercultivar F1 hybrids with respect to traits related to lodicule vascularization

		Lodicule size class		Vascular tissue (mm)		*P*-value		
Crosses	Assortment: HvAP2/*Sac*I	Small	Large	Mean	SD	ANOVA	χ^2 (1:2:1)	χ^2 (3:1)
SV235 × SV223	Homo. SV235	0	29	0.41	0.02	1.52*E*-20	0.29	0.13
	Hetero. F1	42	0	0.14	0.01			
	Homo. SV223	20	0	0.07	0.00			
SV235 × SV230	Homo. SV235	0	21	0.47	0.01	8.77*E*-45	0.45	0.20
	Hetero. F1	42	0	0.10	0.00			
	Homo. SV230	28	0	0.05	0.00			

extent of their vascularization was similar to that in a non-cleistogamous cultivar (Nair *et al.* 2010), but in contrast, there was no perceptible vascularization in either KNG or SV230 lodicules (Figure 1, A and D). Vascular bundles were plentiful within the transparent portion of the SV235 × KNG F_1 lodicule, but were absent from its opaque portion (Figure 1, A and B). While the transparent portion enlarged markedly during the progression to anthesis (Figure 1C), the volume of the opaque portion remained largely unchanged. As a result, the two different portions of the lodicule remained readily distinguishable (Figure S1). The SV235 × SV230 F_1 hybrid lodicules developed no vascular bundles, nor did they form a transparent portion (Figure 1, D and E). Thus, the presence of either *cly1.b* or *cly1.c* inhibited lodicule vascularization. Lodicules in the florets of both non-cleistogamous cultivars and the wild barley accession OUH602 were highly vascularized, unlike those formed by cleistogamous cultivars (Table 1). [Note that occasionally, the volume of vascular tissue differed between a pair of sister lodicules (Figure S1); in this case, the lodicule having the greater vascularization was taken as representative.] At anthesis, despite some swelling of the lodicules, anther extrusion did not occur in SV235, confirming the observation of Nair *et al.* (2010); at this stage, the lodicules, which were smaller than those formed in AZ, SN, MOR, and BAR (Table 1), were unable to push the lemma and palea apart. However, when the spikes were exposed to 2,4-D, the lodicules expanded by 2.4-fold in depth and by 1.8-fold in width (Figure 1, C and F), sufficient to promote floret gaping and anther extrusion (Figure S2).

Lodicule size and anther extrusion are inherited as dominant traits

The lodicules formed by SV235 × *Cly1.a* F_1 hybrids were as large as those formed by the *Cly1.a* parent (Table 1), they were transparent (Table S2), and anther extrusion was as effective (Table 1); thus for all three traits, the SV235 allele (termed *cly1.b*2; see below) was recessive to *Cly1.a*. When supplied with 2,4- D, anther extrusion in the F_1 hybrids became more pronounced. Since both the extent and volume of lodicule vascularization in the SV235 × KNG F_1 hybrid were intermediate (Figure 1A), the *cly1.b*2 and *cly1.b* alleles act codominantly (Figure 1, B and C, Table 1, and Table S2). However, the F_1 hybrid lodicules did respond to 2,4-D treatment, although insufficiently to induce anther extrusion (Table 1), implying that for this trait, *cly1.b*2 is recessive to *cly1.b*. The remaining *cly1.b*2 × *cly1.b* F_1 hybrids behaved similarly (Table 1). The SV235 × SV230 and SV235 × SV223 F_1 hybrids both formed nonvascularized lodicules (Figure 1D) similar in size to those produced by their *cly1.c* parent (Figure 1E), and neither lodicule size (Figure 1F) nor anther extrusion (Table 1) was responsive to 2,4-D treatment. Thus *cly1.b*2 was recessive to *cly1.c* (Table 1 and Table S2). The lodicules formed by *Cly1.a* × *cly1.b* F_1 hybrids were transparent, their size was similar to those formed by the *Cly1.a* parent, and anther extrusion occurred whether or not 2,4-D was supplied. Thus, as suggested by Nair *et al.* (2010), *cly1.b* is recessive to *Cly1.a*. Similarly, the phenotype of the *Cly1.a* × *cly1.c* F_1 hybrid showed that *cly1.c* is recessive to *Cly1.a* (Table 1 and Table S2). The *Cly1.a* × *cly1.c* F_1 hybrid lodicules were smaller than those formed by *Cly1.a* plants and less vascularized than those formed by either the *Cly1.a* parent or the *Cly1.a* × *cly1.b* F_1 hybrid (Table 1). The inference was that *cly1.c* is a stronger allele than *cly1.b* with respect to the reduction of vascularization. Since the size of *cly1.b* × *cly1.c* F_1 hybrid lodicules was similar to that of both their *cly1.b* and *cly1.c* parents (Table 1), *cly1.b* and *cly1.c* were assumed to be allelic to one another. The *cly1.b* × *cly1.c* F_1 hybrids produced nontransparent lodicules that were nonsensitive to 2,4-D treatment, and anther extrusion failed whether or not 2,4-D treatment was given.

Genetic basis of cleistogamy

The extent of lodicule vascularization varied continuously in the F_2 population derived from the cross SV235 × KNG (Figure 2A). Anther extrusion did not occur in any of the F_2 progeny unless the spikes were exposed to 2,4-D; even then, only a small number of progeny exhibited a modicum of floret gaping. In the F_2 population bred from both the SV235 × SV230 and SV235 × SV223 F_1 hybrids, variation with respect to the extent of transparent tissue in the lodicule was bimodal (Figure 2, B and C); in the former population, 70 progeny produced large lodicules and 21 produced small ones, while in the latter population the ratio was 62:29. Both these segregation ratios are consistent with monogenic inheritance (χ^2 values of, respectively, 0.13 [P = 0.72] and 2.01 [P = 0.15]; see Table 2), with the SV235 allele acting as a recessive. When combined with the marker data, a major QTL (LOD of 11.03) underlying vascular development could be mapped in the SV235 × KNG population to a position flanked by *ABC165* and *ABC153* (Figure 3). The

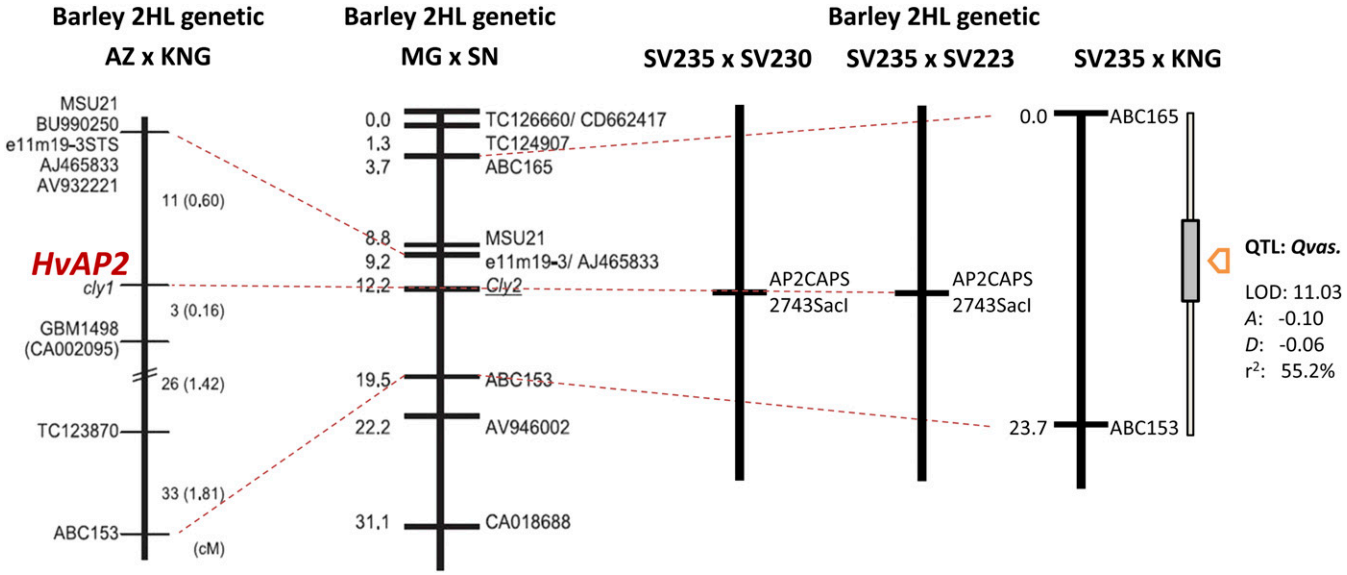

Figure 3 Linkage groups harboring QTL associated with the extent of lodicule vascularization. The shaded box shows the confidence interval associated with the QTL. HvAP2 denotes the CAPS marker AP2CAPS2743SacI that targets a variable nucleotide within the ninth intron of *cly1*. The AZ × KNG and MG (Misato Golden) × SN chromosome arm 2HL genetic maps were generated by Turuspekov *et al.* (2009).

locus, denoted *Qvas*, explained 55.2% of the phenotypic variance. The genomic location of *Qvas* coincided with that of *cly1* (Turuspekov *et al*. 2005, 2009). No other markers in this region were informataive between the parents, nor was there any sequence polymorphism present in the 11.2-kb region surrounding *cly1*. However, the same region was variable between SV235 and both SV230 and SV223 (Table S3). This variation allowed the development of the CAPS marker AP2CAPS2743SacI, which targets a nucleotide in the ninth intron. Homozygosity for the SV235 allele was completely associated with normal vascularization, while homozygosity for the SV230/SV223 allele or heterozygosity was associated with reduced vascular development (Figure 3). The result was consistent with the notion that *cly1* controls vascularization and dominance in the direction of less vascularization.

Transcription of cly1

SV235 and KNG differed with respect to the accumulation of *cly1* transcript in the developing spike (Figure 4A). In the latter cultivar, the abundance of transcript was stable throughout the period spanning the formation of the lemma primordium to the formation of green anthers; however, in SV235, its abundance between the lemma primordium and the awn primordium stage was some two- to fourfold below that present in KNG spikes. As spike development proceeded, *cly1* transcript abundance increased until it reached a level indistinguishable from that present in KNG (Figure 4A). In the SV235 × KNG F_1 hybrid, its abundance was intermediate between the two parents. In SV230, it was two- to threefold higher at the awn primordium and white anther stages than at the earlier developmental stages (Figure 4B) and overall about twofold that in KNG.

miR172-assisted cleavage of cly1.b2 mRNA

The modified 5′ RACE assay showed that *cly1* mRNA cleavage was minimal or absent in both SV235 and KNG (Nair *et al.* 2010). None of the sequenced RACE clones generated from these two cultivars possessed an miR172 target site (Figure 4C). In SV230, two of the 42 clones sequenced did provide evidence of cleavage between the A and U nucleotides known to be the major cleavage site in *Cly1.a* mRNA; the remaining 40 clones were cleaved at other sites.

Bisulfite sequencing of the cly1 promoter region

As shown by bisulfite sequencing, the CpG and CpNpG sites upstream of *cly1* (between −2300 and −245 from the transcription start site) were hypermethylated, but the CpG sites between −244 and +500 were all demethylated (Figure 5A). The methylation status of the −245 cytosine site was correlated with *cly1* transcript abundance (Figure S3). At the stamen primordium stage, the SV235 −245 site was 75% methylated, while the levels at the equivalent KNG, SV230, GP, AZ, and MOR sites were, respectively, 25, 0, 0, 13, and 25%. At the green anther stage, the degree of methylation fell to 25% in SV235, 6% in MOR, and 0% in KNG, SV230, GP, and AZ (Table 3). In the leaf, the levels were 19% in SV235 and 6% in KNG (Table 3).

Characterization of the population of small RNAs

A total of 150 million small RNAs (siRNAs) reads were recovered from the MOR immature spike at the awn primordium stage. Their sequences suggested a possible interaction with *cly1* DNA or mRNA at four positions (Figure 5A). The *cly1* locus includes three sites (–3926 to –3893, –1991 to –1651, and –444 to –178) that could in principle be targeted by siRNAs (Figure 5A). The –444 to –178 site overlapped the

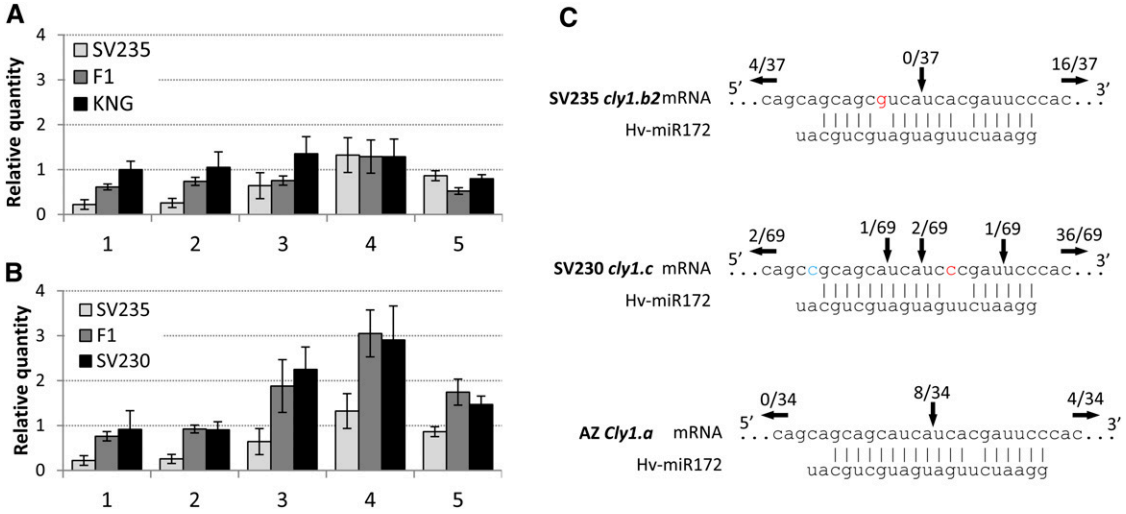

Figure 4 Transcription and miR172-directed degradation of *cly1* in immature spikes. Barley *actin* was used as the reference gene. (A) SV235, KNG, SV235 × KNG F_1 hybrid. (B) SV235, SV230, SV235 × SV230 F_1 hybrid. (1) lemma primordium stage, (2) stamen primordium stage, (3) awn primordium stage, (4) white anther stage, (5) green anther stage. Data shown as mean ± SE of at least three biological replicates. (C) miR172-directed cleavage of *cly1* mRNA assayed by a modified 5′ RACE protocol. Vertical arrows indicate the inferred 5′ termini of miR172-guided cleavage, and the number above each arrow gives the proportion of clones showing these sites. *cly1*.b2 (SV235), *cly1*.b (KNG), *cly1*.c (SV230), *Cly1.a* (AZ).

key –245 cytosine site (Figure 5A). In all, 212 reads matched sequences within the 7.5-kb *cly1* region, and 98% of the reads were specific to the *cly1* region (rather than to any other region in the whole genome sequence), suggesting that the siRNAs were largely transcribed from the *cly1* region. The +3075 to +3097 site contained sequences complementary to the miR172 sequence, demonstrating that miR172 is indeed generated in the immature spike of barley, as proposed by Nair *et al.* (2010).

Transcription pattern of putative ncRNA

Public domain RNA-seq sequence was accessed to identify upstream transcript of *cly1*, but no matches were uncovered. However, a perfect match was obtained with *cly1* coding sequence (data not shown). The abundance of putative noncoding RNA (ncRNA) covering the key −245/−244 CpG site was estimated using 14 primer pairs (Figure S4A). The only one able to generate the expected 136-bp amplicon from a cDNA template was SV235-244RT_600U / SV235-244RT_712L, even though all of the primer pairs amplified successfully from a genomic DNA template. Amplification efficiency was greater from a cDNA template prepared using random priming than from one generated by oligo(dT) priming, indicating that the primary transcript was likely processed *in vivo* (Figure S4B). The abundance of putative lncRNA transcript upstream of *HvAP2* in SV235 was lower than that in KNG, while that in KNG was lower than that in SV230 (Figure S4C).

Discussion

The partial development of the lodicule in SV235 is due to a reduced abundance of cly1 transcript

Although the sequence of the SV235 *cly1* allele suggested that the cultivar should be cleistogamous, its lodicules nevertheless developed detectable vascularization, which permitted some (although insufficient) swelling to occur. Furthermore, the cultivar was able to respond to 2,4-D treatment in the same way as non-cleistogamous cultivars did (Figure 1). The linkage analysis was consistent with the notion that *cly1* was responsible for lodicule vascularization in SV235, since there was no recombination between the phenotype and *cly1* genotype in the *cly1.c* × *cly1.b*2 F_2 population (Figure 2, B and C), and *cly1* colocated with *Qvas* (Figure 3). Because the *cly1* product inhibits lodicule development (Nair *et al.* 2010), the lesser abundance of *cly1* transcript in *cly1.b*2 florets (compared to that in *cly1.b* and *cly1.c* types) was associated with the extent of lodicule development. The inference was that *cly1* must suppress the development of lodicules in barley, just as the rice *AP2* ortholog does (Zhou *et al.* 2012).

DNA methylation within cly1.b2 represses transcription

Although the reduced abundance of *cly1* mRNA in SV235 was responsible for the insufficient development of the SV235 lodicules, no sequence polymorphisms differentiated either the coding or the immediate flanking regions of the gene. *cly1* mRNA was not degraded by miR172-guided cleavage in SV235 and other cleistogamous cultivars (Figure 4C). Although it remains possible that a functional sequence polymorphism exists outside the flanking regions analyzed, a more likely scenario is that SV235 carries an epiallele within its noncoding *cly1* sequence, which has the effect of alleviating the repression of *cly1* transcription. Such epialleles within transcriptional regulatory regions have been repeatedly associated with gene silencing in both plant and mammalian genomes (Shibuya *et al.* 2006; Kinoshita *et al.* 2007; Deng *et al.* 2010; Ecker 2013). In rice, a genome-wide scan of DNA methylation has indicated that CpG methylation is rarest within regions stretching from slightly upstream to some 500 nt downstream of the transcriptional start site (Zemach *et al.*

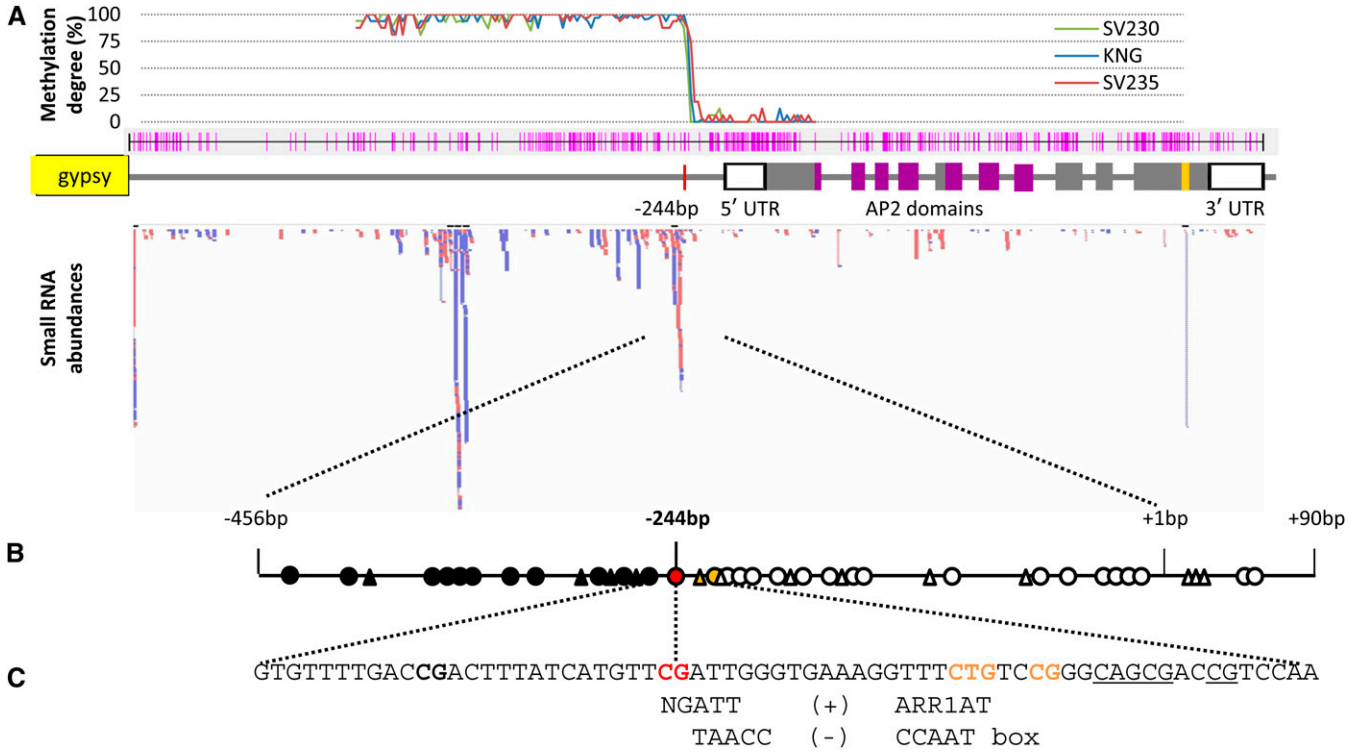

Figure 5 Putative regulatory factors for *cly1*. (A) Global DNA methylation degree related to siRNA frequency. Methylation levels as revealed by the proportion of CpG sites methylated; the pink lines indicate the positions of CpG and CpNpG sites in the upstream and coding regions of *cly1*. The red bars indicate siRNA reads homologous to the *cly1* genomic sequence, and the blue bars show complementary reads. (B) DNA methylation in the upstream region of *cly1*. Solid circles indicate hypermethylated CpG sites, the red circle identifies the CpG site correlated with *cly1* transcription, and open circles show demethylated CpG sites; solid triangles indicate methylated CpNpG sites and open ones nonmethylated CpNpG sites. (C) Putative *cis* elements. NGATT: an ARR1 binding element (+ strand). TAACC: a CCAAT box (− strand).

2010). The key −245 cytosine site (Figure 5A) lies within this region; this site was differentially methylated in the cultivars tested. A possible mechanism via which the −245 site could become differentially methylated may involve an interaction between the site and either small or lncRNAs. In plants, small (21–24 nt) RNAs are known to trigger epigenetic gene silencing (Lang-Mladek *et al.* 2010; Hauser *et al.* 2011). The *cly1* locus includes four sites, including the −245 site, which could in principle be targeted by siRNAs (Figure 5A). Thus it is feasible that either siRNA or lncRNA may act in *cis* with methylation, especially as a large number of the short RNA reads originated from immediately upstream of the −245 site (Figure S4). Some of the siRNAs and lncRNAs plausibly represent degraded or processed transcripts of the −444 to −178 region. The siRNAs may be able to methylate their own coding sequences. The key −245/−244 CpG site is located within a motif homologous to a putative protein-binding element in the *Arabidopsis thaliana* ARR1 protein (Figure 5B), a cytokinin-responsive transcriptional activator (Sakai *et al.* 2001). Methylation of the −245 cytosine may therefore prevent the binding of a relevant activator(s), leading to a reduction in *cly1* transcription activity.

cly1.c upregulates cly1 transcription due to the presence of a functional sequence variant

The *cly1.c* allele exerted a particularly strong inhibitory effect on lodicule vascularization (Table 1 and Table S2), probably because of the increased abundance of *cly1* mRNA present during the period between the awn primordium and the white anther stages. *cly1.c* was dominant over *cly1.b*2 (Table S2) with respect to both *cly1* transcription and lodicule volume. The sequences differ by a C/T substitution at the −245 site, which may result in some derepression of transcription governed by DNA methylation (Table S3), and possibly also in the enhanced accumulation of *cly1* mRNA. The *cly1.c* sequence also included a mismatch with the miR172 target site at 6 nt downstream of the key polymorphism in *cly1.b*, but this variant did not appear to affect the stability of *cly1* mRNA and the miR172 duplex (Vallone and Butler 2004), so could not explain the difference in lodicule development induced by *cly1.b* and *cly1.c* (Figure 4). A further sequence polymorphism between *cly1.c* and *cly1.b* was located at position 4462 (within the first exon; see Table S3), producing a T49M polymorphism. The T variant is present in both *cly1.c* (cleistogamous) and *Cly1.a* (non-cleistogamous) types (Nair *et al.* 2010), so cannot have any effect on lodicule development.

Origin and potential application of the various cly1 alleles

To date, four alleles have been identified at *cly1*. In cultivars carrying *Cly1.a*, the lodicules become vascularized and are responsible for the non-cleistogamy phenotype. This allele is

Table 3 DNA methylation at the key −245 cytosine site in immature spikes and leaves

Cultivar	Allele	No. of clones								miR172-assisted mRNA cleavage	Vascular tissue
		Stamen primodium stage			Green anther stage			Leaf			
		Nonmethylated	Methylated	%	Nonmethylated	Methylated	%	Nonmethylated	Methylated	%	
SV235	*cly1.b2*	4	12	75	12	4	25	16	3	19	Not cleaved	Partially developed
KNG	*cly1.b*	12	4	25	16	0	0	16	1	6	Not cleaved	Not developed
SV2308[a]	*cly1.c*	—	—	—	—	—	—	—	—	—	Not cleaved	Not developed
GP	*cly1.b*	16	0	0	16	0	0	n.t., not tested	n.t.		n.t.	Not developed
AZ	*Cly1.a*	14	2	13	16	0	0	n.t.	n.t.		Cleaved (Nair *et al.* 2010)	Developed
Morex	*Cly1.a*	12	4	25	15	1	6	n.t.	n.t.		n.t.	Developed

[a] Sequence variance (C/T) replaced CG site in SV230.

dominant over each of *cly1.b*, *cly1.b*2, and *cly1.c*. The allelism of *cly1.b* and *cly1.c* suggested by Nair *et al.* (2010) was confirmed here (Table 1). The *cly1.b* and *cly1.c* sequences are thought to have evolved independently, one in northern Europe and the other in the western part of the Mediterranean basin. Their differential function became apparent when the flowering behavior of *cly1.b* × *cly1.b*2 and *cly1.c* × *cly1.b*2 F_1 hybrids was contrasted. That *cly1.b*2 is probably a variant of *cly1.b* was demonstrated by identifying that both alleles are tightly linked to *Qvas* (Figure 3). As *cly1.b* and *cly1.b*2 share the same DNA sequence over an 11.2-kb region including the complete coding sequence, the likelihood is that the latter evolved from the former following an epigenetic event.

The application of 2,4-D to spikes of *cly1.b*2 carriers induced floret gaping and anther extrusion, thereby offering the possibility of manipulating flower type by the simple expedient of spraying with 2,4-D. In the context of F_1 hybrid grain production, fully open flowering is necessary for both pollen dispersal and cross-pollination. The *cly1.b*2 allele offers a practical means of controlling flowering type in F_1 hybrids involving two carriers of *cly1.b*2. A 2,4-D application supplied prior to anthesis should encourage the non-cleistogamy needed for F_1 hybrid grain production, while the F_1 hybrid plants themselves are cultivated normally and so remain cleistogamous. Closed flowering is advantageous as it limits the entry of certain pathogens (in particular *Fusarium* head blight fungus) and inhibits pollen-derived gene flow (important in the context of genetically modified varieties).

Acknowledgments

We thank Takayuki Yazaya for mapping small RNA reads and gene annotation. This research was funded by grants made to T.K. by the Japanese Ministry of Agriculture, Forestry and Fisheries (Genomics for Agricultural Innovation grant no. TRG1004 and Genomics-based Technology for Agricultural Improvement grant no. TRS1002).

Literature Cited

Briggs, D., 1978 *Barley*. Chapman & Hall, London.

Deng, Y., B. Yu, Q. Cheng, J. Jin, H. You *et al.*, 2010 Epigenetic silencing of WIF-1 in 4 hepatocellular carcinomas. J. Cancer Res. Clin. Oncol. 136: 1161–1167.

Ecker, J. R., 2013 Epigenetic trigger for tomato ripening. Nat. Biotechnol. 31: 119–120.

Hauser, M. T., W. Aufsatz, C. Jonak, and C. Lushchning, 2011 Transgenerational epigenetic inheritance in plants. Biochim. Biophys. Acta. Gene Regul. Mech. 1809: 459–468.

Honda, I., Y. Turuspekov, T. Komatsuda, and Y. Watanabe, 2005 Morphological and physiological analysis of cleistogamy in barley (*Hordeum vulgare*). Physiol. Plantarum 124: 524–531.

Kapoor, M., A. Baba, K. Kubo, K. Shibuya, K. Matsui *et al.*, 2005 Transgene-triggered, epigenetically regulated ectopic expression of a flower homeotic gene pMADS3 in Petunia. The Plant Journal 43: 649–661.

Kenan-Eichler, M., D. Leshkowitz, L. Tal, E. Noor, C. Melamed-Bessudo *et al.*, 2011 Wheat hybridization and polyploidization results in deregulation of small RNAs. Genetics 188: 263–272.

Kinoshita, Y., H. Saze, T. Kinoshita, A. Miura, W. J. J. Soope *et al.*, 2007 Control of FWA gene silencing in *Arabidopsis thaliana* by SINE-related direct repeats. Plant J. 49: 38–45.

Kirby, E. J. M., and M. Appleyard, 1981 *Cereal Development Guide*. National Agricultural Centre, Kenilworth, England.

Komatsuda, T., I. Nakamura, F. Takaiwa, and S. Oka, 1998 Development of STS markers closely linked to the vrs1 locus in barley, *Hordeum vulgare*. Genome 41: 680–685.

Kurauchi, N., T. Makino, and S. Hirose, 1994 Inhieritance of cleistogamy-chasmogamy in barley. Barley Genet. Newsl. 23: 19.

Lang-Mladek, C., O. Popova, K. Kiok, M. Berlinger, B. Rakic *et al.*, 2010 Transgenerational inheritance and resetting of stress-induced loss of epigenetic gene silencing in Arabidopsis. Mol. Plant 3: 594–602.

Langmead, B., C. Trapnell, M. Pop, and S. L. Salzberg, 2009 Ultrafast and memory-efficient alignment of short DNA sequences to the human genome. Genome Biol. 10: R25.

Livak, K. J., and T. D. Schmittgen, 2001 Analysis of relative gene expression data using real-time quantitative PCR and the $2^{-\Delta\Delta}C_T$ Method. Methods 25: 402–408.

Mayer, K. F. X., R. Waugh, P. Langride, T. J. Close, R. P. Wise *et al.*, 2012 A physical, genetic and functional sequence assembly of the barley genome. Nature 491: 711–716.

Nair, S. K., N. Wang, Y. Turuspekov, M. Pourkheirandish, S. Sinsuwongwat *et al.*, 2010 Cleistogamous flowering in barley arises from the suppression of microRNA-guided HvAP2 mRNA cleavage. Proc. Natl. Acad. Sci. USA 107: 490–495.

Ning, S. Z., N. Wang, S. Sakuma, M. Pourkheirandish, J. Z. Wu *et al.*, 2013 Structure, transcription and post-transcriptional regulation of the bread wheat orthologs of the barley cleistogamy gene Cly1. Theor. Appl. Genet. 126: 1273–1283.

Saisho, D., M. Pourkheirandish, H. Kanamori, T. Matsumoto, and T. Komatsuda, 2009 Allelic variation of row type gene Vrs1 in barley and implication of the functional divergence. Breed. Sci. 59: 621–628.

Sakai, H., T. Honma, T. Aoyama, S. Sato, T. Kato *et al.*, 2001 ARR1, a transcription factor for genes immediately responsive to cytokinins. Science 294: 1519–1521.

Simonov, A. V., and T. A. Pshenichnikova, 2012 Chromosomal localization of the speltoidy gene, introgressed into bread wheat from *Aegilops speltoides* Tausch., and its interaction with the Q gene of *Triticum spelta* L. Russ. J. Genet. 48: 1120–1127.

Simons, K. J., J. P. Fellers, H. N. Trick, Z. C. Zhang, Y. S. Tai *et al.*, 2006 Molecular characterization of the major wheat domestication gene Q. Genetics 172: 547–555.

Trapnell, C., L. Pachter, and S. L. Salzberg, 2009 TopHat: discovering splice junctions with RNA-Seq. Bioinformatics 25: 1105–1111.

Turuspekov, Y., Y. Mano, I. Honda, N. Kawada, Y. Watanabe *et al.*, 2004 Identification and mapping of cleistogamy genes in barley. Theor. Appl. Genet. 109: 480–487.

Turuspekov, Y., N. Kawada, I. Honda, Y. Watanabe,, and T. Komatsuda, 2005 Identification and mapping of a QTL for rachis internode length associated with cleistogamy in barley. Plant Breeding 124: 542–545.

Turuspekov, Y., I. Honda, Y. Watanabe, N. Stein,, and T. Komatsuda, 2009 An inverted and micro-colinear genomic regions of rice and barley carrying the cly1 gene for cleistogamy. Breed. Sci. 59: 657–663.

Vallone, P. M., and J. M. Butler, 2004 AutoDimer: a screening tool for primer-dimer and hairpin structures. Biotechniques 37: 226–231.

Wang, N., S. Z. Ning, M. Pourkheirandish, I. Honda, and T. Komatsuda, 2013 An alternative mechanism for cleistogamy in barley. Theor. Appl. Genet. 126: 2753–2762.

Wang, S., C. J. Basten, and Z.-B. Zeng, 2012 *Windows QTL Cartographer 2.5*. Department of Statistics, North Carolina State University, Raleigh, NC.

Zemach, A., I. E. Mcdaniel, P. Silva, and D. Zilberman, 2010 Genome-wide evolutionary analysis of eukaryotic DNA methylation. Science 328: 916–919.

Zhou, Y., D. F. Lu, C. Y. Li, J. H. Luo, B. F. Zhu *et al.*, 2012 Genetic control of seed shattering in rice by the APETALA2 transcription factor SHATTERING ABORTION1. Plant Cell 24: 1034–30 1048.

Communicating editor: R. S. Poethig

GENETICS

Supporting Information
http://www.genetics.org/lookup/suppl/doi:10.1534/genetics.114.171652/-/DC1

An Epiallele at *cly1* Affects the Expression of Floret Closing (Cleistogamy) in Barley

Ning Wang, Shunzong Ning, Jianzhong Wu, Akemi Tagiri, and Takao Komatsuda

DOI: 10.1534/genetics.114.171652

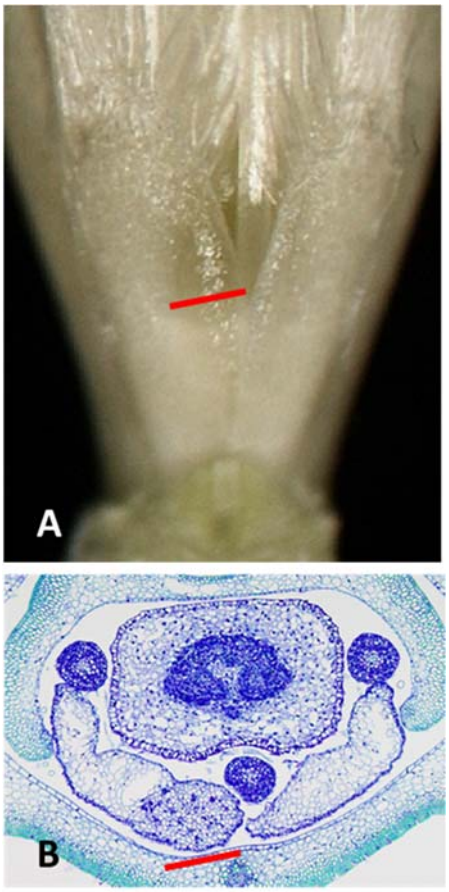

Figure S1 Measuring lodicule vascularization from (A) stereomicroscope images and (B) transverse sections from the same floret. The width of transparent tissue (red line) correlates with the volume of vascularized tissue.

Figure S2 Anther extrusion in SV235 at anthesis. (A) Untreated spikes, (B) spikes exposed to 100 ppm 2,4-D for three days.

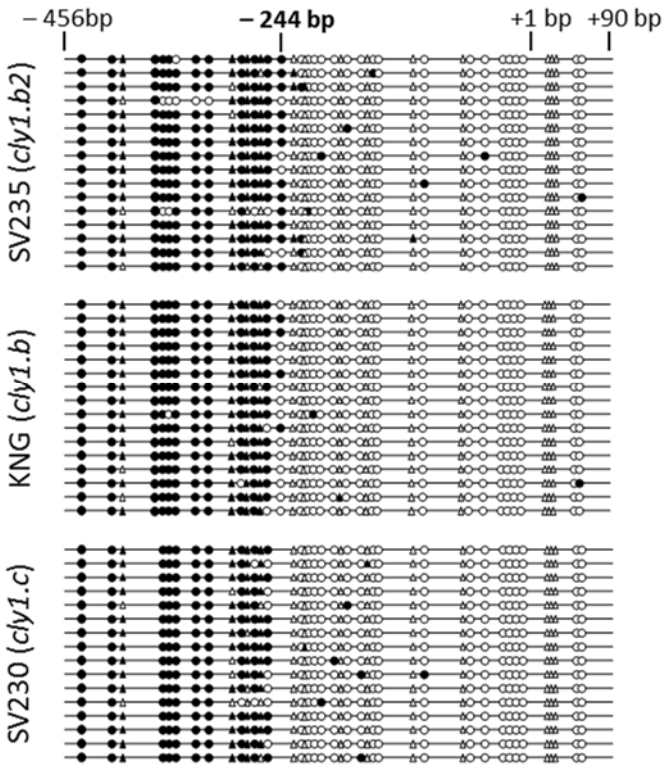

Figure S3 DNA methylation at CpG sites in the upstream region of *cly1*. Methylation level within a specific upstream region revealed the key –245/–244 CpG site. Filled circles indicate methylated CpG sites and empty ones non-methylated CpG sites; filled triangles indicate methylated CpNpG sites and empty ones non-methylated CpNpG sites.

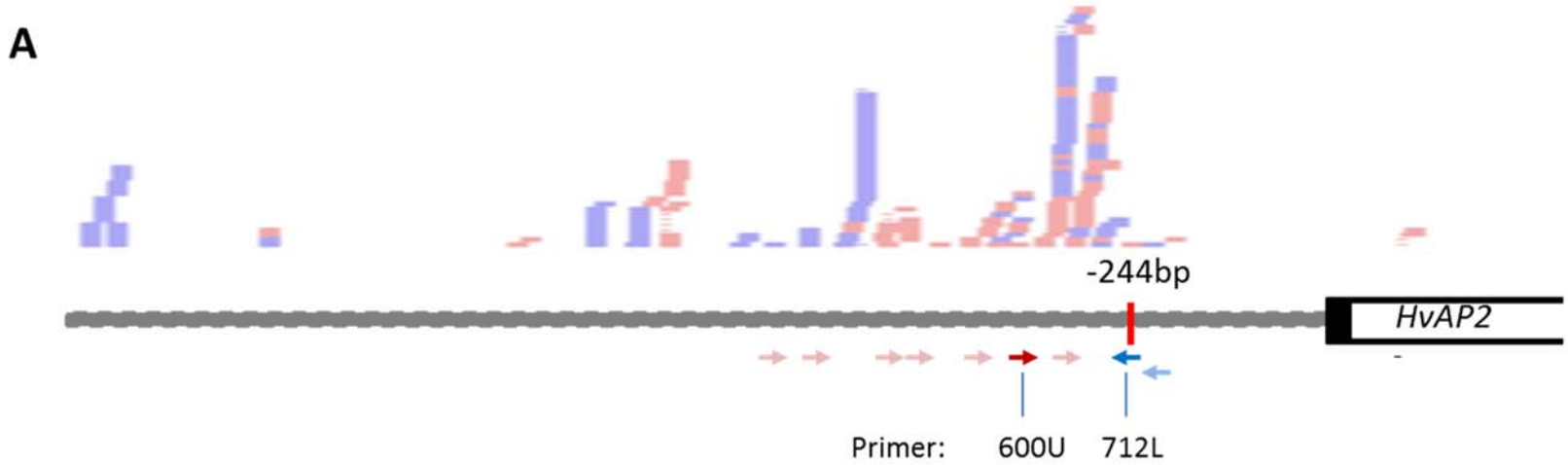

B

	SV235		KNG		Morex	
Stage	2	3	2	3	2	3
RT (Random primer)	+	+	+	+	+	+
RT (oligo dT primer)	?	?	?	?	+	?
Actin +RT (+ Control)	+	+	+	+	+	+
Actin -RT (- Control)	-	-	-	-	-	-

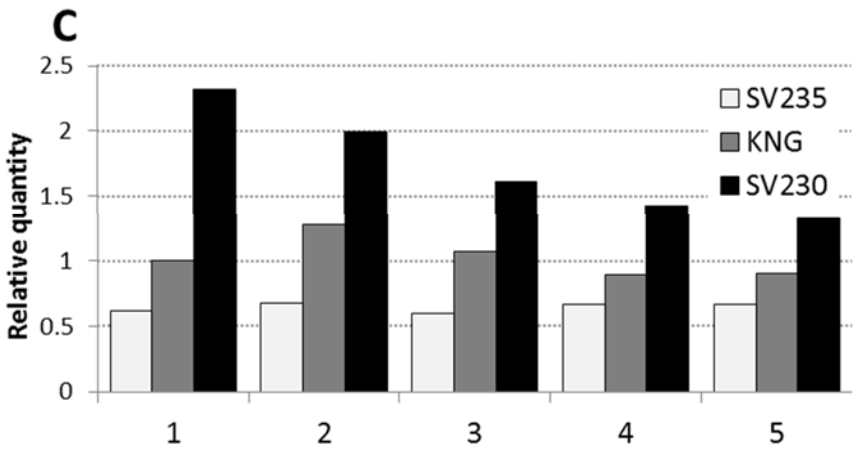

Figure S4 Transcription of putative lncRNA from the upstream sequence of *cly1*. Stages assayed as given in the legend to Fig. 4. Barley *actin* was used as the reference gene. (A) All the primer combinations generated a clear amplicon from genomic DNA template, but the pair SV235-244RT_600U / SV235-244RT_712L was the only one to successfully amplify from cDNA template. (B) A comparison between cDNA template produced using an oligo dT primer and a random primer for lncRNA detection. Stage 2, stamen primordium stage; stage 3, awn primordium stage. ?: no clear amplification, +: clear amplicon, –: no amplicon. Actin: *actin* fragment amplicon from cDNA template produced using an oligo dT primer. (C) Relative abundance of SV235 (light gray bar), KNG (dark gray bar) and SV230 (black bar) message. KNG stage 1 (lemma primordium) was used as the reference sample for quantification. Data shown derived from the mean of at least three biological replicates.

Tables S1-S3

Available for download as Excel files at http://www.genetics.org/lookup/suppl/doi:10.1534/genetics.114.171652/-/DC1.

Table S1 Sequences of PCR primers targeted at *cly1*.

Table S2 Dominance relationships for alleles determining the volume of transparent tissue in the lodicule.

Table S3 Location of inter-cultivar sequence polymorphisms within an 11.2 kb region encompassing *cly1*.